Robust H Current Control of Three-Phase Grid-Connected Voltage Source Converters Using Linear Matrix Inequalities

Gholami-Khesht, Hosein; Davari, Pooya; Novak, Mateja; Blaabjerg, Frede

Published in:
Proceedings of the 2021 IEEE 22nd Workshop on Control and Modelling of Power Electronics (COMPEL)

DOI (link to publication from Publisher):
10.1109/COMPEL52922.2021.9646071

Publication date:
2021

Document Version
Accepted author manuscript, peer reviewed version

Robust H_∞ Current Control of Three-Phase Grid-Connected Voltage Source Converters Using Linear Matrix Inequalities

Hosein Gholami-Khesht
AAU Energy
Aalborg University
Aalborg, Denmark
hgk@energy.aau.dk

Pooya Davari
AAU Energy
Aalborg University
Aalborg, Denmark
pda@energy.aau.dk

Mateja Novak
AAU Energy
Aalborg University
Aalborg, Denmark
nov@energy.aau.dk

Frede Blaabjerg
AAU Energy
Aalborg University
Aalborg, Denmark
fbl@energy.aau.dk

***Abstract*— This paper proposes a robust H_∞ current control of a three-phase LCL-filtered grid-connected voltage source converter (VSC). As main contributions, new modeling for three-phase grid-connected VSC is presented that considers control input delay and grid impedance variations. The linear matrix inequalities (LMIs) formulation and polytopic type uncertainty representation are employed to achieve this goal. The performance of the proposed control strategy is investigated under different grid short circuit ratios (SCRs). Simulation and experimental results confirm the excellent performance of the proposed control method under different grid conditions.**

Keywords—Grid-connected voltage source converter, Robust H_∞ current control, Linear matrix inequalities, Weak grids.

I. INTRODUCTION

Three-phase LCL-filtered grid-connected voltage source converters (VSCs) can be found in many different power system applications such as renewable energies-based distributed power generation systems, high-voltage direct current (HVDC) transmission systems and flexible alternating current transmission systems (FACTS) due to their fast dynamic response, full controllability and flexibility. These power converters employ many control loops, including outer power (or voltage) control loops and inner current control loops, to satisfy the defined tasks and control objectives. The current control loop is an essential part of the control system, providing sufficient damping for LCL filter resonance, eliminating grid voltage disturbances, reducing the negative impact of control delay and grid impedance uncertainties, and generating sinusoidal current under stringent international standards according to power quality. Different control structures have been reported to fulfill these power and control objectives, among them proportional-integral (PI) and proportional-resonant (PR) control methods [1]–[4], model predictive control (MPC) method [5]–[9], and robust H_∞ control method [10]–[20] are frequently used methods.

Particularly, the ability to overcome the plant uncertainties and disturbance challenges makes H_∞ methods attractive and powerful solutions for power system applications. They are based on the state-space model of the system and provide a systematic and straightforward way to calculate the robust control gains. Recently, they are found in many power system applications such as stand-alone [10]–[15] and grid-connected converters [16]–[20]. In [16], [17], an H_∞ current control based on the LMIs formulation is proposed for a grid-connected VSC. It can consider the uncertainty in the grid impedance on the system stability. And as an exciting feature, all proportional and resonant control gains are calculated systematically and straightforwardly. However, the control input delay was not yet considered in the design procedure, which uses the continuous-time state-space model [15]. Moreover, only control system performance under strong grid conditions or higher short circuit ratios (SCR>5) is studied in [16]–[19]. Because most stability issues and performance degradation usually happen under weak grid conditions with low SCR (SCR< 2) as the penetration level of power converters increases, they cannot be identified if only high short circuit ratios are considered in system performance validation.

In this respect, this paper proposes a new H_∞ robust current control method based on the LMI formulation. A full expression of the control input delay (and not its approximation) and polytopic representation of grid inductance uncertainties are considered in the control system design based on the Lyapunov-Krasovskii function [21]. Moreover, the feasibility of the proposed control method is examined in weak grid conditions, which is not considered so far. A detailed comparison between the proposed and different other presented robust H_∞ control methods is presented in Table I. As it can be seen, all previously presented works guarantee closed-loop stability mathematically. Moreover, they can ensure good reference tracking and proper disturbance rejection. On the other hand, the important differences are how they can consider system uncertainties and deal with the control input delay.

The rest of this paper is organized as follows. Section II presents the dynamics of an LCL-filtered grid-connected VSC. Section III gives more information on the proposed robust H_∞ current control method, including weighting functions selection, generalized state-space model representation, and control gain calculation based on the LMI formulation. Section IV provides simulation and experimental results in a three-phase 5 kW laboratory setup, evaluating the effectiveness of the proposed control strategy

Ref.	Reference tracking	Disturbance Rejection		Parameter uncertainties	Control Delay	Stability analysis	Control gain minimization	Time domain	Application	
		Liner	Nonlinear						Stand-alone	Grid-connected
[10]	+	+	−	+	−	+	−	Con.	+	−
[11]	+	+	−	+	−	+	+	Dis.	+	−
[12]	+	+	+	+	−	+	−	Con.	+	−
[13]	+	+	−	+	+	+	−	Dis.	+	−
[14]	+	+	+	−	+	+	+	Dis.	+	−
[15]	+	+	+	−	−	+	−	Con.	+	−
[16]	+	+	+	+	+	+	+	Dis.	−	Strong Grid
[17]	+	+	+	+	+	+	+	Dis.	−	Strong Grid
[18]	+	+	+	+	+	+	+	Dis.	−	Strong Grid
[19]	+	+	+	+	−	+	+	Dis.	−	Strong Grid
Proposed	+	+	+	+	+	+	+	Con.	−	Weak and Strong Grid

Con.: Continuous, Dis.: Discrete

under different power system conditions. Finally, section V concludes the paper.

II. System Description and Equations

Fig. 1 shows a schematic diagram of the three-phase LCL-filtered VSC alongside the proposed control method. The system state-space equation considering the control input delay $(\tau(t))$ and Kirchhoff's Laws can be written as:

$$\dot{x}(t) = A_c x(t) + B_c u(t-\tau(t)) + D_c v_g(t) \tag{1}$$

where, $x = [x_1\ x_2\ x_3] = [i_f\ v_c\ i_g]$ is the state vector. v_c, v_g, and u are the capacitor, grid, and inverter output voltages. i_f and i_g are the inverter and grid currents. $\tau(t)$ is the time-varying input delay $\tau(t) \in [0, t_d]$. Also, A_c, B_c, and D_c are state and input matrixes as follows:

$$A_c = \begin{bmatrix} 0 & \frac{-1}{L_f} & 0 \\ \frac{1}{C} & 0 & \frac{-1}{C} \\ 0 & \frac{1}{L_g} & 0 \end{bmatrix}, B_c = \begin{bmatrix} \frac{1}{L_f} \\ 0 \\ 0 \end{bmatrix}, D_c = \begin{bmatrix} 0 \\ 0 \\ \frac{-1}{L_g} \end{bmatrix}, \tag{2}$$

$$L_g = L_{g1} + L_{g2}$$

here, L_f, L_{g1} and C are the inverter side and grid side filter inductances and filter capacitance to filter the PWM (pulse-width modulation) harmonics. L_{g2} is a grid inductance seen from the PCC, which is uncertain and can vary due to the change in the power system conditions.

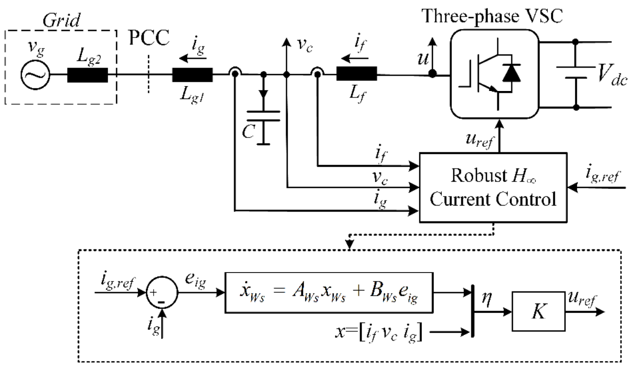

Fig. 1. Three-phase LCL-filtered grid-connected voltage source converter under the proposed H_∞ current controller.

III. Proposed Robust H_∞ Current Controller

In the proposed control method, the desired stability and performance requirements and control input limitation are considered in the design step as weighting functions. A performance weighting function (W_S) defines the sensitivity loop function requirements, and a constant control input weighting factor (W_{KS}) is considered to limit the control gain as follows:

$$W_S = \frac{y}{e_{ig}} = \sum_{n=1,5,7} \frac{k_{sn}\left(s + \xi\omega_n\right)}{s^2 + \omega_n^2},\ W_{KS} = k_u \tag{3}$$

here, $e_{ig} = i_g - i_{g,ref}$ is the current tracking error, ω_n is a resonant frequency, ξ damping factor, and k_{sn} and k_u are constant gains. The performance weighting function provides an infinite gain at the resonant frequency, ensuring zero tracking error and complete disturbance rejection of sinusoidal signals. It is worth noting that in this study resonators at fundamental, fifth, and seventh components are considered. Moreover, a constant gain is selected for the control input weighting, limiting the control gains while not increasing the controller order.

W_S in (3) can be written in state-space representation as:

$$\dot{x}_{Ws}(t) = A_{Ws} x_{Ws}(t) + B_{Ws} e_{ig}(t) \tag{4}$$

By including weighting functions in the plant state-space model, Eqs. (1)-(4) give the generalized state-space model as:

$$\begin{cases} \dot{\eta} = A\eta + Bu(t-\tau(t)) + Dw \\ z = C_1\eta + D_{12}u(t-\tau(t)) + D_{11}w \end{cases} \tag{5}$$

here, η contains the plant states in (1) and states related to the state-space representation of (4). z and w are the penalty vector (or regulated output) and external inputs (references and disturbances).

A. H_∞ Control Gain Calculations Based on Delay Dependent LMIs

The main goal is to find a robust state feedback control gain (K) that internally stabilizes the closed-loop system in (5) with the time-varying input delay $\left(\tau(t) \in [0, t_d], \dot{\tau}(t) \le d < 1\right)$ and leads to L_2-gain less than γ:

$$\min_{K\ stabilizing} \|T_{zw}\|_\infty = \frac{\|z\|_{\ell 2}}{\|w\|_{\ell 2}} < \gamma \quad (6)$$

Note that d is a constant that assign the delay maximum variation rate. The following proposition can solve the above optimization problem based on the LMI formulation and Lyapunov-Krasovskii function.

Proposition: Given $\gamma > 0, t_d > 0, 0 \le d < 1$ and a tuning parameter $\varepsilon > 0$, if there exist matrices $\overline{P} > 0, \overline{P}_2 > 0, \overline{Q} > 0, \overline{R} > 0, \overline{S} > 0$ such that (7) is met. Then the robust static feedback control gain (K) and the control input (u(t)) can be calculated as:

$$\begin{cases} K = Y\overline{P}_2^{-1} \\ u(t) = K\eta(t) \end{cases} \quad (8)$$

It is worth noting that the LMIs of the proposition in (7) are affine of L_g, meaning that the value and variation rate of L_g is uncertain, but it is bounded by:

$$L_{g,\min} \le L_g \le L_{g,\max} \quad (9)$$

Therefore the control gain in (8) guarantees the system robust stability and performance in the presence of the grid inductance uncertainties if the LMI is jointly satisfied for minimum and maximum values of grid inductances ($L_{g,min}$ and $L_{g,max}$). Moreover, notice that LMI in (7) is delay-dependent due to time delay information (t_d, d). Also, LMI not only depends on the maximum time delay but also its variation. Indeed, (7) guarantees the system stability and performance for the time delay in an interval $\left(0 \le \tau(t) < t_d\right)$ with a rate variation lower than d $\left(\dot{\tau}(t) \le d < 1\right)$.

The presented proposition can be proven based on the following Lyapunov-Krasovskii function and some manipulations as well as mathematical simplifications:

$$\begin{cases} V(t,\eta,\dot{\eta}) = \eta^T P \eta + \int_{t-t_d}^{t} \eta^T(s) S \eta(s) ds + \\ \int_{t-\tau(t)}^{t} \eta^T(s) Q \eta(s) ds + t_d \int_{-t_d}^{0}\int_{t+\theta}^{t} \dot{\eta}^T(s) R \dot{\eta}(s) ds d\theta > 0 \\ \dot{V} + z^T z - \gamma^2 w^T w < 0 \end{cases}$$
$$P > 0, S > 0, Q > 0, R > 0 \quad (10)$$

where, relationship $\overline{X} = \overline{P}_2^T X \overline{P}_2$, $\left(X = P, R, S, Q, S_{12}\right)$ exist between matrices in (7) and (10). The complete proof of (7) and (10) is ignored here. However, the interested reader can refer to the following reference [21] for more details.

IV. Simulation and Experimental Verification

The performance of the proposed control method is investigated through several simulation and experimental tests. The experiment includes a three-phase 5-kW PWM-VSC, a constant DC voltage supply, LCL filter, grid simulator, and a DS1007 dSPACE system. Simulations have been carried out on a MATLAB Simulink model with the same parameters as in the experiments. The system parameters are given in Table II.

Fig. 2 shows the steady-state grid currents and tracking errors under different grid SCRs (SCR=1 and 7). As shown, the sinusoidal current generation and approximately zero tracking errors are obtained under different grid conditions. The obtained waveforms confirm the feasibility and good performance of the proposed robust H_∞ current controller over a wide range of grid SCR variations, including weak grid conditions.

The steady-state grid currents under a distorted grid voltage and weak grid condition (SCR=1.27) are examined in Fig. 3. Despite the grid voltage is including 5% of the fifth and seventh components (or total harmonic distortion (THD_v) equal to 7.1%), the proposed robust current control method can successfully generate the sinusoidal currents and meet the international standards like IEEE 1547 (THD_i=1.1%).

Table II: System and control parameters of grid-connected VSC.

Power system parameters		**Control parameters**	
Nominal power (P_n)	5 [kW]	Performance weighting function	
Nominal line voltage (v_g)	173 [V]	ω	100π
Filter capacitor (C)	30 [µF]	ξ	2
Inverter-side inductor (L_f)	1.5 [mH]	k_{s1}	40
Grid-side inductor (L_g)	1.9-19 [mH]	k_{s5}, k_{s7}	4
DC-link voltage (V_{dc})	600 [V]	Control input weighting factor	
Sampling time (T_S)	100 µs	k_u	0.001

$$\begin{bmatrix} & | & D & \overline{P}_2^T C_1 \\ \overline{\varphi} & | & \varepsilon D & 0 \\ & | & 0 & 0 \\ & | & 0 & Y^T D_{12}^T \\ - & - & - & - \\ * & | & -\gamma^2 I_{2\times 2} & D_{11}^T \\ * & | & D_{11} & -I \end{bmatrix} < 0, \begin{bmatrix} \overline{R} & \overline{S}_{12} \\ * & \overline{R} \end{bmatrix} > 0, \overline{\varphi} = \begin{bmatrix} \overline{\varphi}_{11} & \overline{P} - \overline{P}_2 + \varepsilon \overline{P}_2^T A^T & \overline{S}_{12} & BY + \overline{R} - \overline{S}_{12} \\ * & -\varepsilon \overline{P}_2 - \varepsilon \overline{P}_2^T + t_d^2 \overline{R} & 0 & \varepsilon BY \\ * & * & -\left(\overline{S} + \overline{R}\right) & \overline{R} - \overline{S}_{12}^T \\ * & * & * & -(1-d)\overline{Q} - 2\overline{R} + \overline{S}_{12} + \overline{S}_{12}^T \end{bmatrix} \quad (7)$$

$$\overline{\varphi}_{11} = A\overline{P}_2 + \overline{P}_2^T A^T + \overline{S} + \overline{Q} - \overline{R}$$

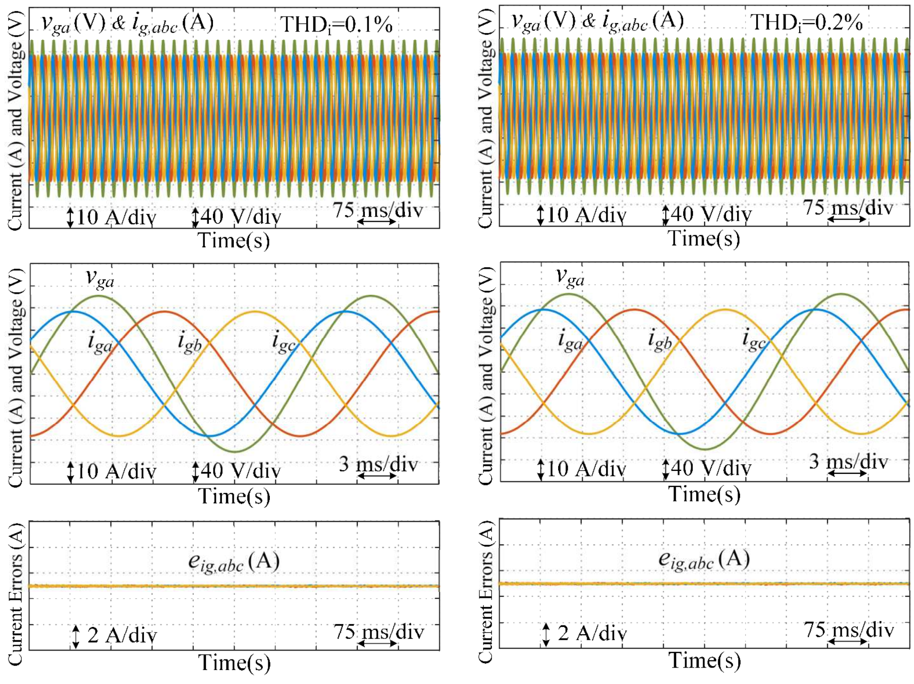

(a)

(b)

Fig. 2. Simulated steady-state performance of the grid currents under different grid SCRs, (a) SCR=1 and L_g=19mH (P=5 kW, Q= -3.3 kVar), and (b) SCR=7 and L_g=2.7 mH (P=5 kW, Q=0 kVar).

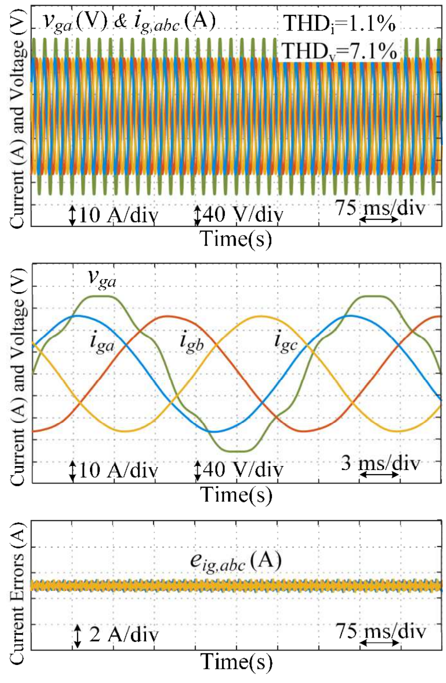

Fig. 3. Simulated steady-state performance of the grid currents under distorted grid voltage (SCR=1.26, L_g=15mH, P=5 kW, and Q= -2.5 kVar).

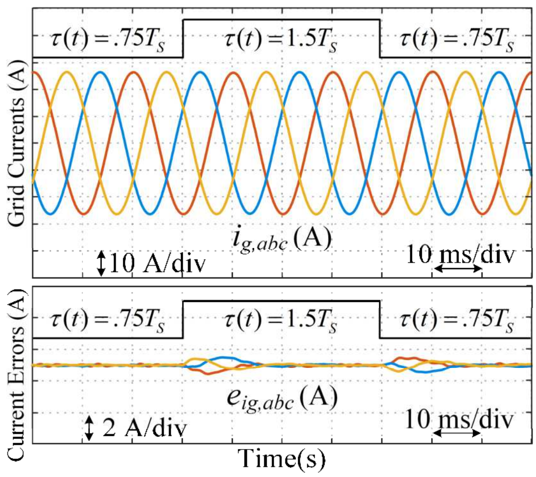

Fig. 4. Simulated steady-state performance of the grid currents under distorted grid voltage (SCR=1.26, L_g=15mH, P=5 kW, and Q= -2.5 kVar).

Fig 4. studies the robustness of the proposed control method under variable control delays, demonstrating the analytical results obtained based on the Lyapunov-Krasovskii function. As shown, when the control delay is increased from $0.75T_S$ to $1.5T_S$ and then back to $0.75T_S$. However, under these step changes, the system remains stable.

The transient and start-up response of grid currents under step change in the reference current are examined in Fig. 5, while different grid SCRs (SCR=1 and 7) are considered. They confirm a fast dynamic response without any overshoots under uncertain grid SCRs. However, under the lower grid SCR, the system response is a little slower due to a larger grid inductance. It is worth remarking that for this test, the active power under both cases is the same, but the reactive power to keep the capacitor voltage at an acceptable level differs under different grid SCRs.

Finally, Fig. 6 shows the transient performance of the proposed robust H_∞ current control method under a step change of the reference current under two different grid SCRs in practice. Experimental results confirm a good transient response and sinusoidal current generation over a wide range of grid SCR variations. The experiments validate the previous obtained analytical results and simulations.

V. CONCLUSION

This paper proposed the design and experimental verification of a new robust H_∞ current control for the grid-connected VSCs. In the proposed control method, control input delay, grid voltage disturbance, grid SCR variations, control gain minimization, and tracking of sinusoidal signals are considered mathematically and simultaneously. Simulations and experiments confirm the effectiveness of the proposed control method over a wide range of grid SCR variations, including weak grid conditions, which have not been examined by similar control strategies so far.

ACKNOWLEDGMENT

The work is supported by the Reliable Power Electronic-Based Power System (REPEPS) project at the AAU Energy, Aalborg University as a part of the Villum Investigator Program funded by the Villum Foundation.

REFERENCES

[1] F. Hans, W. Schumacher, S.-F. Chou, and X. Wang, "Design of multifrequency proportional-resonant current controllers for voltage-source converters," *IEEE Trans. Power Electron.*, pp. 1–1, May 2020.

[2] M. Lu, A. Al-Durra, S. M. Muyeen, S. Leng, P. C. Loh, and F. Blaabjerg, "Benchmarking of stability and robustness against grid

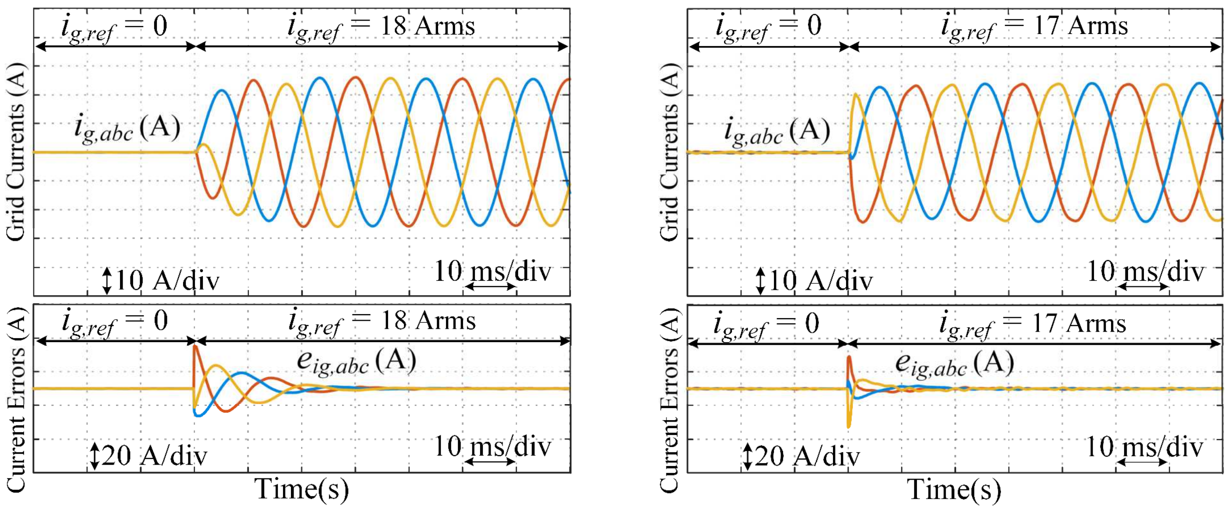

(a) (b)

Fig. 5. Simulated transient performance of the grid currents under different grid SCRs, (a) SCR=1.26 and L_g=15 mH (P=4.5 kW, Q=-3 kVar), and (b) SCR=7 and L_g=2.7 mH (P=5 kW, Q=1 kVar).

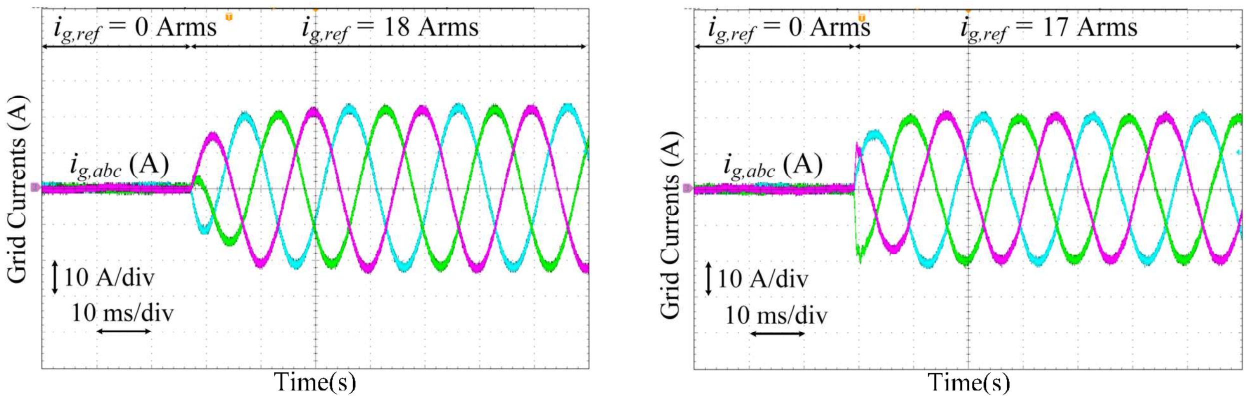

(a) (b)

Fig. 6. Measured transient response of the grid currents, (a) SCR=1.26 and L_g=15 mH (P=4.5 kW, Q=-3 kVar), and (b) SCR=7 and L_g=2.7mH (P=5 kW, Q=1 kVar).

impedance variation for LCL-filtered grid-interfacing inverters," *IEEE Trans. Power Electron.*, vol. 33, no. 10, pp. 9033–9046, Oct. 2018.

[3] S. Zhou et al., "An improved design of current controller for LCL-type grid-connected converter to reduce negative effect of PLL in weak grid," *IEEE J. Emerg. Sel. Top. Power Electron.*, vol. 6, no. 2, pp. 648–663, Jun. 2018.

[4] H. Gholami-Khesht, M. Monfared, and S. Golestan, "Low computational burden grid voltage estimation for grid connected voltage source converter-based power applications," *IET Power Electron.*, vol. 8, no. 5, pp. 656–664, May 2015.

[5] C. S. Lim, S. S. Lee, Y. C. Cassandra Wong, I. U. Nutkani, and H. H. Goh, "Comparison of current control strategies based on FCS-MPC and D-PI-PWM control for actively damped VSCs with LCL-filters," *IEEE Access*, vol. 7, pp. 112410–112423, Aug. 2019.

[6] P. Falkowski and A. Sikorski, "Finite control set model predictive control for grid-connected AC-DC converters with LCL filter," *IEEE Trans. Ind. Electron.*, vol. 65, no. 4, pp. 2844–2852, Apr. 2018.

[7] X. Zhang, L. Tan, J. Xian, H. Zhang, Z. Ma, and J. Kang, "Direct grid-side current model predictive control for grid-connected inverter with LCL filter," *IET Power Electron.*, vol. 11, no. 15, pp. 2450–2460, Dec. 2018.

[8] A. M. Bozorgi, H. Gholami-Khesht, M. Farasat, S. Mehraeen, and M. Monfared, "Model predictive direct power control of three-phase grid-connected converters with Fuzzy-based duty cycle modulation," *IEEE Trans. Ind. Appl.*, vol. 54, no. 5, pp. 4875–4885, 2018.

[9] H. Gholami-Khesht, P. Davari, and F. Blaabjerg, "An adaptive model predictive voltage control for LC-filtered voltage source inverters," *Appl. Sci.*, vol. 11, no. 2, 2021.

[10] T. S. Lee, S. J. Chiang, and J. M. Chang, "H_∞ loop-shaping controller designs for the single-phase UPS inverters," *IEEE Trans. Power Electron.*, vol. 16, no. 4, pp. 473–481, 2001.

[11] G. Willmann, D. F. Coutinho, L. F. A. Pereira, and F. B. Líbano, "Multiple-loop H-infinity control design for uninterruptible power supplies," *IEEE Trans. Ind. Electron.*, vol. 54, no. 3, pp. 1591–1602, 2007.

[12] L. F. A. Pereira, J. V. Flores, G. Bonan, D. F. Coutinho, and J. M. G. da Silva, "Multiple resonant controllers for uninterruptible power supplies—a systematic robust control design approach," *IEEE Trans. Ind. Electron.*, vol. 61, no. 3, pp. 1528–1538, Mar. 2014.

[13] J. S. Lim, C. Park, J. Han, and Y. Il Lee, "Robust tracking control of a three-phase DC-AC inverter for UPS applications," *IEEE Trans. Ind. Electron.*, vol. 61, no. 8, pp. 4142–4151, 2014.

[14] S. P. Ribas, L. A. Maccari, H. Pinheiro, R. C. de L. F. Oliveira, and V. F. Montagner, "Design and implementation of a discrete-time H-infinity controller for uninterruptible power supply systems," *IET Power Electron.*, vol. 7, no. 9, pp. 2233–2241, Sep. 2014.

[15] W. Ma, S. Ouyang, J. Zhang, and W. Xu, "Control strategy based on H_∞ repetitive controller with active damping for islanded microgrid," *IEEE Access*, vol. 7, pp. 162157–162168, 2019.

[16] G. G. Koch, L. A. Maccari, R. C. L. F. Oliveira, and V. F. Montagner, "Robust H∞ state feedback controllers based on linear matrix inequalities applied to grid-connected converters," *IEEE Trans. Ind. Electron.*, vol. 66, no. 8, pp. 6021–6031, 2019.

[17] G. G. Koch, C. R. D. Osorio, H. Pinheiro, R. C. L. F. Oliveira, and V. F. Montagner, "Design procedure combining linear matrix inequalities and genetic algorithm for robust control of grid-connected converters," *IEEE Trans. Ind. Appl.*, vol. 56, no. 2, pp. 1896–1906, 2020.

[18] L. A. Maccari *et al.*, "LMI-based control for grid-connected converters with LCL filters under uncertain parameters," *IEEE Trans. Power Electron.*, vol. 29, no. 7, pp. 3776–3785, Jul. 2014.

[19] R. Bimarta and K. H. Kim, "A robust frequency-adaptive current control of a grid-connected inverter based on LMI-LQR under polytopic uncertainties," *IEEE Access*, vol. 8, no. Lcl, pp. 28756–28773, 2020.

[20] L. Huang, H. Xin, and F. Dorfler, "H_∞-control of grid-connected converters: design, objectives and decentralized stability certificates," *IEEE Trans. Smart Grid*, vol. 11, no. 5, pp. 3805–3816, Sep. 2020.

[21] E. Fridman, "Introduction to time-delay systems," Birkhäuser Basel, 2014.